Journal of Materials Chemistry C

Accepted Manuscript

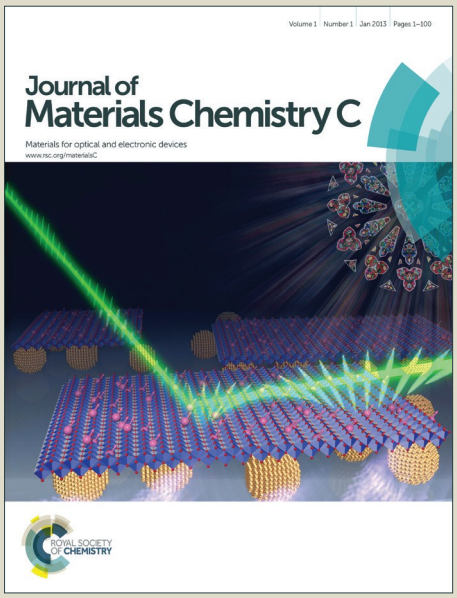

ROYAL SOCIETY OF CHEMISTRY

www.rsc.org/materialsC

View Article Online
DOI: 10.1039/C6TC01103A

Photosensitive chiral self-assembling materials: significant effects of small lateral substituents

Martin Cigl,[a,b] Alexey Bubnov,[a] Miroslav Kašpar,[a] František Hampl,[b] Věra Hamplová,[a] Oliva Pacherová[a] and Jiří Svoboda[b]

[a] *Institute of Physics, The Czech Academy of Sciences, Na Slovance 1999/2, CZ-182 21 Prague 8, Czech Republic*

[b] *Department of Organic Chemistry, University of Chemistry and Technology, CZ-166 28 Prague 6, Czech Republic*

Novel azobenzene-based photosensitive mesogens with lactate chiral unit were synthesized. In order to modify the rate of the thermal *Z-E* isomerization of these compounds, small lateral substituents were introduced into their core in the proximity of the azo group. The influence of lateral substitution on the kinetics of the *Z-E* isomerization, mesomorphic behaviour, and UV-Vis absorption spectra was studied. It was found that the position of the substituents in the azobenzene core significantly affects the rate of their thermal isomerization. The stability of *Z*-isomers of several studied compounds is comparable to that of compounds with a complex molecular structures designed for optical data storage. Although lateral substitution influences the breadth/length ratio of the core, liquid-crystalline properties of the studied materials have been preserved.

Introduction

Photosensitive materials which can change their structural and optical properties in response to light irradiation as an external stimulus are intensively studied due to their high application potential in photonics. Photonic devices combine utilization of photons and electrons for signal processing which brings many advantages. The most significant ones are e.g. higher signal to noise ratio, faster data processing or multiple channel processing. Such materials can be used for construction of devices like spatial optical modulators (holography)[1,2], high density data storage[3] media and many other devices based on molecular switches.[4] Because of the increasing requirements on volume and speed of data processing, searching for materials enabling construction of the above mentioned devices has become an important area in the field of materials chemistry. In this respect, azobenzene structural unit represents the most intensively studied type of photosensitive moiety used in such materials. In addition to photonics, its reversible *E*/*Z* photoisomerization has been utilized as a light triggered switch in a variety of soft actuators[5–7], sensors[8], optical[9] and biomedical systems.[10,11]

View Article Online
DOI: 10.1039/C6TC01103A

A number of photonic applications can be set up on soft self-assembling materials, i.e. liquid crystals (LCs)[12-15], utilizing their functional fluidity combined with the short range orientation ordering that results in their self-organizing nature. Usually, alignment of liquid crystals can be changed by external stimuli like electric field or temperature. In addition, involving the photosensitive azobenzene moiety (either present in a substance doped in LC matrix or incorporated in the molecular core of LC) external light irradiation can serve as a cheap, clean and easy-guided stimulus.[16]

Despite the fact that azobenzene derivatives are one of the most intensively studied photosensitive systems, some drawbacks still persist. They do not form a bi-stable switching system, since the photogenerated *Z*-form thermally re-isomerizes (thermal relaxation) to the thermodynamically more stable *E*-form even in the dark. The rate of this first order process strongly depends on the substitution pattern of the azobenzene moiety.[17,18] Moreover, practical applications require advanced systems exhibiting either extremely fast thermal recovery (systems for data processing) or suppressed thermal relaxation (systems for data storage). Systems exhibiting fast recovery are usually based on push-pull type azobenzenes, i.e. azobenzenes bearing electron donor group and electron withdrawing group in 4 and 4′-positions resp. (also referred as pseudostilbenes[19]). One important disadvantage of such a system is that the particular substitution patterns of derivatives (mostly commercial azo dyes) with reasonably fast thermal relaxation usually disable their incorporation into the molecular core of a liquid crystal. Therefore these compounds are mostly utilized as photochromic guests in LC hosts. Numerous such dye-doped systems have been studied so far[20,21] but they still suffer from either low solubility of the azo dye in the LC host or aggregation of dye molecules during switching cycles. Much effort has also been spent on development of azo compounds with a long living *Z*-isomer suitable for data storage applications.[22] A typical way to increase the stability of *Z*-configuration involves an introduction of steric hindrance in the proximity of azo group by means of bulky lateral substituents[23] or by bridging the azobenzene moiety thus forming cyclic or macrocyclic structures.[24] In some special cases, the *Z*-isomer becomes even thermodynamically more stable than the *E*-isomer and thermal relaxation proceeds in opposite direction.[25,26] However, the introduction of bulky substituents into the molecular core of rod-like LC may lead to the destabilization of mesophases or even to the loss of mesomorphic behavior.[27] Therefore these bulky structures can serve as photochromic guests only, just like azo compounds with fast thermal relaxation. As stated above, such host-guest systems suffer with many problems.

View Article Online
DOI: 10.1039/C6TC01103A

Unlike the above cited studies dealing mainly with complex macrocyclic structures requiring sophisticated multi-step syntheses, we have recently studied[28] photosensitive chiral azo compound **Ia** (see Fig. 1 for the general structure) with a simple molecular structure exhibiting rich mesomorphism in a broad temperature interval. Mesogen **Ia** represents a typical push-pull type azobenzene. Owing to their non-symmetric electron distribution, these substances possess a longitudinal dipole moment which makes them very useful building blocks of LC-cores.[15] Push-pull azobenzene derivatives have been reported as substances exhibiting relatively fast thermal *Z-E* relaxation[22,29] and therefore unsuitable for data storage applications. A question appeared on the possibility of tuning the rate of thermal *Z-E* relaxation. The finding that mesomorphic behaviour is maintained even in the presence of lateral methyl substituent in the molecular core[28] inspired us to design and study a series of novel liquid crystalline materials **Ib-Ii** possessing two identical lateral substituents (CH_3, F Cl, Br) attached in *ortho* positions to azo linkage in one of the aromatic units. It was reasonable to assume that a substitution in the close vicinity of the azo linkage in LCs of general formula **I** may substantially influence the rate of their thermal *Z-E* isomerization due to steric and electronic effects of the substituents. To the best of our knowledge, no similar investigation of the influence of the push-pull azobenzenes substitution on their relaxation has been performed yet.

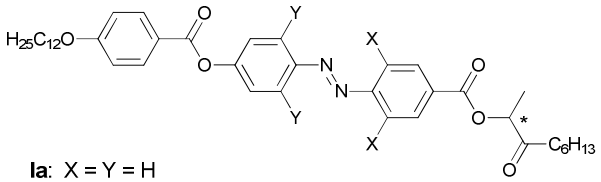

Ia: X = Y = H
Ib: X = H, Y = CH_3
Ic: X = H, Y = Br
Id: X = H, Y = Cl
Ie: X = H, Y = F
If: X = CH_3, Y = H
Ig: X = Br, Y = H
Ih: X = Cl, Y = H
Ii: X = F, Y = H

Fig. 1 Chemical structure of the studied compounds.

Experimental

Materials

The general synthetic route for the synthesis of compounds **Ib-h** is shown in Scheme 1. Compound **Ii** was synthesized in somewhat different way, reported in the Scheme S4 in the supporting information file. Ethyl 4-aminobenzoate **1** and phenols **6**, **7** and **10** were purchased from Sigma-Aldrich and Acros Organics. The non-substituted material **Ia** was synthesized according to the reported procedure.[28] Aminobenzoic acids[30] **2-5** and phenols[31,32] **8** and **9** were obtained by modification of known synthetic procedures. All azobenzene derivatives **11b-i** were prepared following the azo coupling procedure. In the next step, the hydroxy

View Article Online
DOI: 10.1039/C6TC01103A

group of compounds **1b-h** was protected in a form of methyl carbonate by a reaction with methyl chloroformate to yield the protected acids **12a-g**. Then, the chiral terminal chain was introduced by acylation of hexyl (*S*)-lactate with the chlorides of acids **11a-g**. The carbonate protecting group of **13a-g** was removed by hydrolysis with aq. ammonia to release the phenols **14a-g**. Finally, the phenols **14-g** were coupled with 4-(dodecyloxy)benzoic acid in a DCC-mediated reaction to yield the target compounds **Ia-g**. The detailed syntheses and structural characterization of all intermediates and target compounds are summarized in the supporting information file.

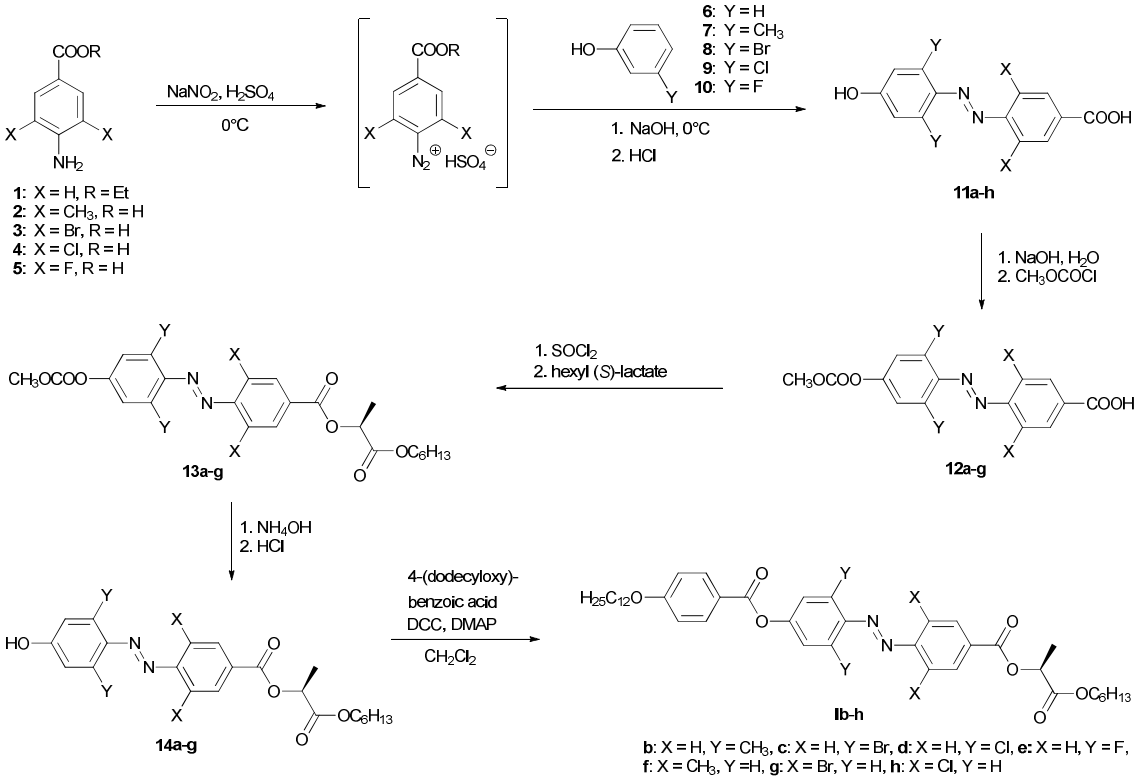

Scheme 1. Synthesis of compounds **Ib-h**.

Kinetic measurements

Kinetics of the thermal *Z*-*E* isomerizations were investigated using NMR spectroscopy, starting from photostationary states. These were achieved by irradiation of the 10 mM solutions of the studied compounds in $CDCl_3$ in quartz cuvettes with a low-pressure mercury lamp (8 W sterilair BLB-8, 366 nm) equipped with a filter. The changes of integral intensities of several well-separated signals of *E* and *Z*-isomer were periodically monitored maintaining the same phasing of the spectra (see supporting information file for details).

The acquired *Z*-isomer mole fraction time dependencies were fitted by the least square procedure to the equation 1:

View Article Online
DOI: 10.1039/C6TC01103A

$$\ln\left(\frac{x_0}{x_\tau}\right) = k\tau \qquad (1)$$

where x_0 and x_τ are mole fractions of the *Z*-isomer at the time $\tau = 0$ and at the time τ, respectively; k is the rate constant of the thermal *Z-E* relaxation. Equation corresponds to the linearized form of a general first order rate equation. The reported rate constants are averages of the values obtained from at least three measurements. Activation parameters were obtained from Arrhenius plot of rate constants measured at least at three different temperatures in the span from 20 °C to 50 °C.

UV-Vis spectra

UV-Vis spectra were recorded using Shimadzu UV-VIS spectrometer 1601. Spectra of 20 μM solutions in chloroform were taken at room temperature in quartz cuvettes of optical length 1 cm.

Mesomorphic and structural properties

Observation of the characteristic textures and their changes by polarizing optical microscopy (POM) was carried out in 12 μm thick glass cells, which were filled with LC material in the isotropic phase by means of capillary action in dark. The inner surfaces of the glass plates were covered by Indium-Tin-Oxide electrodes and polyimide layers unidirectionally rubbed, which ensures planar alignment of the molecules. A LINKAM LTS E350 heating/cooling stage with TMS 93 temperature programmer which enabled temperature stabilization within ±0.1 K was used for temperature control. Phase transition temperatures, melting points (m.p.), clearing points (c.p.) and phase transition enthalpies (ΔH) were determined by differential scanning calorimetry (DSC - Pyris Diamond Perkin-Elmer 7) on samples of 4-8 mg hermetically sealed in aluminium pans in cooling/heating runs in a nitrogen atmosphere at a heating/cooling rate of 5 K min^{-1}. The temperature was calibrated on extrapolated onsets of melting points of water, indium and zinc. The enthalpy change was calibrated on enthalpies of melting of water, indium and zinc.

Small angle X-ray scattering (SAXS) measurements have been performed to determine structural properties of the identified mesophases. Bruker D8 DISCOVER SUPER SPEED device with rotating Cu anode (wavelength λ = 1.5418Å) working with 12 kW power and equipped with the elements as follows: the parabolic Göbel mirror conditioning the incident beam and the soller slits, the LiF monochromator and the scintillation detector on the side of the diffracted beam has been used for the studies. The Anton Paar chamber DCS 350 has been used for the temperature control (accuracy in temperature stabilization is 0.1 K). The positions

View Article Online
DOI: 10.1039/C6TC01103A

of the peaks and the intensity were determined by a computational simulation using Bruker EVA 13 software. For compounds possessing smectic phases, the layer thickness, *d*, has been determined using Bragg's law $n\lambda = 2dsin\theta$, where *d* is calculated from the position of the small angle ($\theta = 0.2^{o}$–4.5^{o}) diffraction peaks.

Results and discussion

Thermal *Z-E* isomerization

There are two widely accepted mechanisms of the azobenzene thermal *Z-E* isomerization.[29] The first one is the rotational pathway via a transition state with a single bond between nitrogen atoms (Fig. 2, pathway a). The second one involves the inversion of the NNC angle through a transition state with a *sp*-hybridized nitrogen atom (Fig. 2, pathway b). Polarization of the N=N bond typical for push-pull azobenzenes increases the rate of the thermal *Z-E* isomerization since it stabilizes the charge separation in transition states of both pathways.[29,33] We expected that steric hindrance of the substituents in *ortho* positions to the azo linkage combined with their electronic effects may considerably influence the rate of thermal relaxation of *Z*-isomers. However, there were limitations for the choice of lateral substituents, especially as far as their size was concerned – they should not supress the ability of the substances to form mesophases. Therefore, the following set of substituents was involved into our study: methyl group combining steric hindrance with a weak positive inductive effect and halogens (F, Cl, Br) as electron withdrawing substituents with variable size. Iodine was omitted because of possible photolability of iodinated materials.

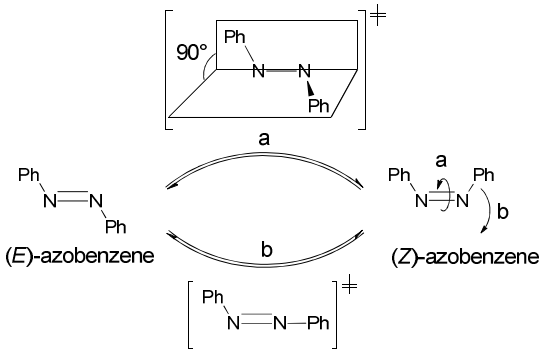

Fig. 2 Isomerization of azobenzene: (a) rotation pathway, (b) inversion pathway.

The course of thermal *Z-E* isomerization fits very well the first-order reaction kinetics. As examples, the linearized plots of isomerizations performed at 20 °C according to Eqn. 1 are shown in Fig. 3. All the obtained kinetic data (the rate constants and activation parameters) of the thermal *Z-E* isomerization in chloroform for all the studied compounds **Ia-Ii** are

View Article Online
DOI: 10.1039/C6TC01103A

summarized in Table 1. For better clearness, half-lives of isomerizations are given as well. Since the kinetics of thermal isomerization comprises of two most likely simultaneously operating pathways with different kinetic parameters, the data in Table 1 represent overall kinetic parameters of the isomerization process. The data unambiguously corroborate our assumption on the influence of lateral substitution on the rate of thermal *Z-E* isomerization.

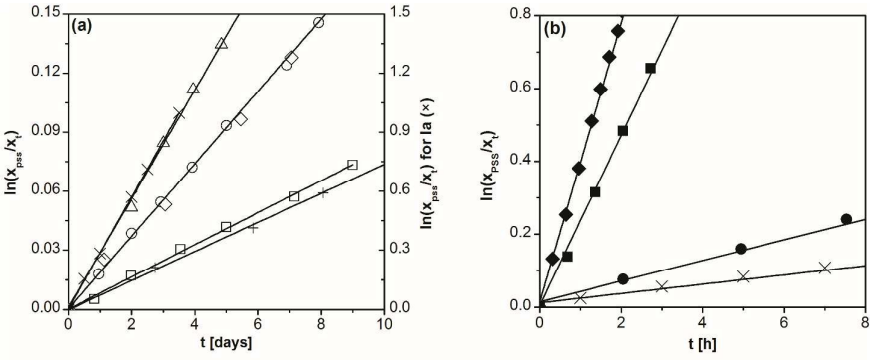

Fig. 3 First order plots for thermal *Z-E* isomerization at 20 °C: (a) **Ia** (×), **Ib**(○), **Ic**(◊), **Id**(□) **Ie**(+), **Ii**(Δ); (b) **Ia** (×), **If**(●), **Ig** (♦), **Ih**(■). Solid lines are fits to eqn. 1.

Depending on the substituent and its position, the rate constants of thermal *Z-E* relaxation vary in the span of almost five orders of magnitude (Table 1). Lateral substitution in *ortho* positions of the *p*-benzoyloxy ("push") ring of the azobenzene moiety decelerates substantially the *Z-E* relaxation. The observed slowing down is a resultant of steric and electronic effects of the substituents. In the case of dimethyl-derivative **Ib** the deceleration can be attributed to steric hindrance. Among the dihalo-derivatives **Ic-Ie** the maximum slowing down was found in the case of dichloro- and difluoro-derivatives **Id** and **Ie**, respectively. We suppose it is the electron-withdrawing effect of these substituents supressing the charge separation in the transition state of thermal relaxation[29,33] which is a predominant factor responsible for the observed decrease in the reaction rate. On the other hand, electron-withdrawing substituents (Br and Cl) in the ring possessing "pull" ester function facilitate the thermal *Z-E* isomerization of materials **Ig** and **Ih** due to their stabilizing effect on charge separation in the transition state. However, relaxation of the difluoro-derivative **Ii** is much slower in comparison with that of the unsubstituted derivative **Ia**. Most likely, the positive mesomeric effect of fluorine compensates its negative inductive effect as ensues from its σ_m and σ_p Hammett constants values[34] (0.34 and 0.06, respectively).

Table 1 Kinetic parameters of thermal *Z-E* isomerization.

View Article Online
DOI: 10.1039/C6TC01103A

comp.	k_{20} [s^{-1}]	E_a [kJ/mol]	log$A$ [s^{-1}]	*x(Z)$_{PSS}$	$t_{1/2}$ (20°C)
Ia	$3.6 \cdot 10^{-6}$	88.8	10.4	0.84	53.5 h
Ib	$2.2 \cdot 10^{-7}$	107.8	12.6	0.74	36.5 days
Ic	$2.2 \cdot 10^{-7}$	103.7	11.7	0.52	36.5 days
Id	$9.7 \cdot 10^{-8}$	97.2	10.3	0.52	82.7 days
Ie	$9.5 \cdot 10^{-8}$	106.2	11.9	0.74	84.4 days
If	$7.9 \cdot 10^{-6}$	101.2	13.3	0.70	24.4 h
Ig	$1.1 \cdot 10^{-4}$	94.2	12.8	0.57	1.8 h
Ih	$7.0 \cdot 10^{-5}$	99.1	13.5	0.43	2.8 h
Ii	$3.6 \cdot 10^{-7}$	113.1	13.7	0.63	22.3 days

* molar fraction of *Z*-isomer at photostationary state

Despite of the remarkable effect of the lateral substituents on isomerization rates, typical increase in activation energy (E_a) as a consequence of lateral substitution was lower than 20 kJ mol^{-1} (except of the fluorinated mesogen **Ii** with 24.3 kJ mol^{-1}). Unfortunately, because of the correlation between E_a and *log A* given by the fact that they were obtained simultaneously from the Arrhenius equation, it is difficult to decide, whether there is a trend between E_a and any substituent parameter.

At this place, it must be stated that the rate constant values measured in solution can be considered as a good estimation of the values measured in mesophases.[18,35] It was already mentioned above, that the thermal stability of the *Z*-isomers is a crucial factor for optical data storage applications of azo compounds.[22] Thermal stability of *Z*-isomers of derivatives **Ib-Ie** was found to be comparable with that found for compounds of complex molecular structure designed as materials for optical data storage[23,36–42] (Table 2). From this point of view our results are of high value considering that all the studied derivatives **Ia-Ii** belong to a push-pull type of azo-compounds where a fast thermal *Z-E* relaxation is expected. It must also be mentioned that all materials given in Table 2 exhibited only a small solvent effect on the observed rate constants.[33] This makes the comparison of the half-lives in different solvents reasonable.

Table 2. *Z*-isomer half-lives compared with published materials.

comp.	$\tau_{1/2}$ (25°C) [days]	solvent	Ref.
Ib	17.0	chloroform	
Ic	20.0	chloroform	
Id	38.7	chloroform	
Ie	35.8	chloroform	
azophane 1	13.7	acetonitrile	36
azophane 2	371.4	toluene	37
tBuBBAB	40.1	solid film	38
azopeptide	27.7	chloroform	39
macrocycle	7.0	THF	40

View Article Online
DOI: 10.1039/C6TC01103A

xanthene hinge	1637.3	toluene	41
2,2´,6,6´-tetrai-PrAB	7.4	isooctane	23
4,4´-bis(AcNH)-2,2´,6,6´-tetraMeOAB	14.1	DMSO	42

An indisputable advantage of the reported new materials is the preservation of liquid crystalline behaviour. Therefore they can be used as both photosensitive LCs and photosensitive guest with expected good miscibility with a LC-host. For dichloro-derivative **Id** we have confirmed an excellent compatibility with commercial nematic matrix E48 (Merck).[43] Materials **Ia** and **Id** along with several other laterally substituted azocompounds were also tested as chiral photosensitive dopants for induction of a cholesteric mesophase with a phototunable helix pitch.[43] Although their helical twisting power was low the photoinduced changes of helical pitch were significant and extremely stable due to the suppressed thermal Z-E isomerization and excellent compatibility with nematic host.

Mesomorphic and structural properties

For the studied materials, the sequence of mesophases and phase transition temperatures were determined by characteristic textures and their changes observed in polarizing optical microscope and from DSC measurements. The mesomorphic properties are summarized in Table 3. On cooling from the isotropic phase (Iso), the non-substituted **Ia** compound possesses blue phase (BPII), the chiral nematic (cholesteric) phase (N*), frustrated twist grain boundary smectic A phase (TGB_A), orthogonal paraelectric smectic A* phase (SmA*), and tilted ferroelectric smectic C* phase (SmC*). Microphotographs of the characteristic textures obtained under crossed polarizers in POM for **Ia** compound are presented on Figure 4.

View Article Online
DOI: 10.1039/C6TC01103A

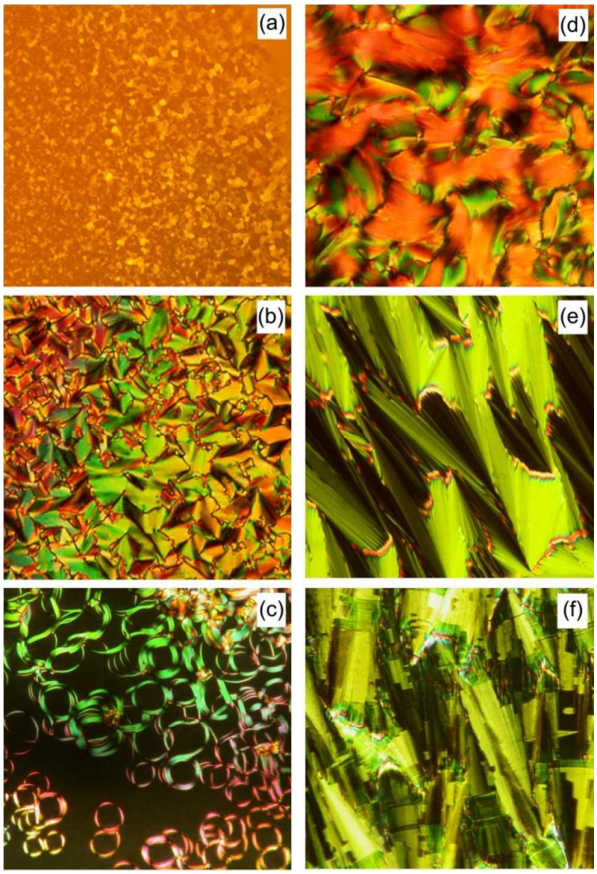

Fig. 4 Microphotographs of the characteristic textures for **Ia** compound: (a) platelet texture of the BPII phase; (b) cholesteric fan-shaped texture; (c) filament texture at the TGBA*-SmA* phase transition; (d) texture of the TGBA* phase; (e) fan-shaped texture of the SmA* phase; (f) broken fan texture of the SmC* phase. All microphotographs (a-b) and (d-f) were obtained on 4 μm thick sample cell with planar alignment; microphotograph (c) was obtained on a one-surface-free sample. Width of all the microphotographs is about 150 μm.

Lateral substitution by methyl group, bromine and chlorine atom at different positions of the molecular core strongly affects the mesomorphic behaviour. Independently on the type and place of the lateral substituent, the melting point and clearing point significantly decreases with respect to that of the non-substituted **Ia** compound. Similar behaviour in the case of laterally substituted compounds with different molecular core has already been reported.[44–47] All the compounds possessing methyl group (**Ib**, **If**) or chlorine atom (**Id**, **Ih**) as a lateral substituent exhibit the orthogonal paraelectric SmA* phase down to room temperature. The lateral substitution by bromine atom close to the chiral centre makes the ferroelectric SmC* phase preferential down to low temperatures similarly as in ref 48. However, both laterally dibromo-substituted compounds **Ic** and **Ig** possess fully monotropic behaviour.

Table 3 Melting (m.p.) and clearing points (c.p.) on the second heating, as well as the phase transition temperatures (Tc) on the second cooling determined by DSC. All the temperatures

View Article Online
DOI: 10.1039/C6TC01103A

are shown in °C. The corresponding enthalpies [Δ*H*] indicated in square brackets are in kJ/mol. "—" the phase does not exist.

comp.	m.p [Δ*H*]	c.p. [Δ*H*]		Tc [Δ*H*]		Tc [Δ*H*]		Tc [Δ*H*]		Tc [Δ*H*]		Tc [Δ*H*]		Tc [Δ*H*]	
Ia	69 [43.69]	131 [0.55]	**Cr**	54 [-40.25]	**SmC***	94 [-0.04]	**SmA***	120 [-0.01]	**TGB$_A$**	123 [-0.48]	**N***	130 [-0.76]	**BPII**	131 [a]	**Iso**
Ib	44 [39.75]	71 [1.07]	**Tg**	-34 [0.28]	—		**SmA***	48 [-0.01]	**TGB$_A$**	56 [-0.64]	**N***	69 [-1.14]	—		**Iso**
Ic	46 [50.68]	46 [50.68]	**Tg**	-32 [0.24]	**SmC***	42 [-1.01]	—		—		—		—		**Iso**
Id	45 [32.20]	56 [1.28]	**Cr**	21[b] [-47.69]	—		**SmA***	55 [-1.51]	—		—		—		**Iso**
Ie	70.2 [39.83]	52 [36.72]	**Cr**	52 [-36.72]	**SmC***	67.6 [-0.05]	**SmA***	102.7 [-0.80]	—		**N***	110.4 [-0.72]	—		**Iso**
Ie	68 [35.82]	73 [0.79]	**Cr**	14 [-5.43]	—		**SmA***	35 [-0.64]	—		**N***	72.00 [-1.36]	—		**Iso**
If	59 [51.95]	59 [51.95]	**Cr**	32[b] [-39.87]	—		—		—		**N***	55.00 [-0.76]	—		**Iso**
Ig	51 [33.93]	103 [0.23]	**Cr**	31[b] [-30.53]	—		**SmA***	63 [-1.35]	**TGB$_A$**	81 [-0.34]	**N***	101.00 [-0.23]	—		**Iso**
Ii	64.2 [40.12]	111.6 [-1.23]	**Cr**	44.2 [-34.05]	—		—		—		N*	111.60 [-1.23]	—		**Iso**

[a] can be determined from POM only; [b] crystallization occurs on further heating as opposite peak on DSC curve.

To confirm the structure, and hence the type of the mesophases, SAXS measurements have been performed. As an example, the results of SAXS for non-substituted compound **Ia**, namely the temperature dependence of the layer spacing, *d*, and SAXS signal intensity within the whole temperature range of the smectic phases are shown in Figure 5. The compound **Ia** exhibits a slight increase of *d*(T) in the SmA* phase on approaching the phase transition to the SmC* phase which can be explained by the stretching of the aliphatic chains with the temperature decrease. On the SAXS intensity curve there is a drop up at about 120 °C corresponding to the TGB$_A$-SmA* phase transition. In the vicinity of the SmA*–SmC* phase transition, there is a pronounced drop of the SAXS intensity at the SmA*–SmC* phase transition followed by a continuous increase below the phase transition temperature. For about 20 K below the SmA*–SmC* phase transition, there is a decrease in *d* values due to increase of the tilt angle and also due to increasing order of the long molecular axes in the plane of the smectic layers. This decrease is followed by an increase in layer spacing values of the SmC* phase on cooling due to stretching of the aliphatic molecule chains while approaching crystallization.

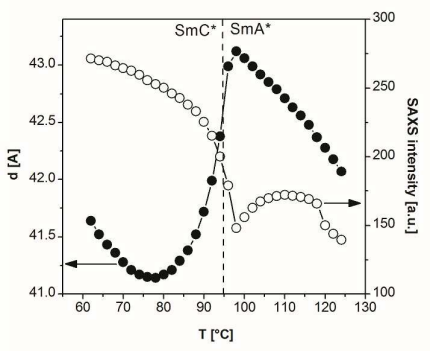

View Article Online
DOI: 10.1039/C6TC01103A

Fig. 5 Temperature dependence of the smectic layer spacing, *d*(T), determined from SAXS measurements and related intensity of the peak maximum for compound **Ia.** The dashed line stands for the temperature of the SmA*- SmC* phase transition on cooling.

UV-Vis spectra

UV-visible spectra of the studied azobenzene derivatives **Ia-Ii** typically show one strong absorption band in the near UV region corresponding to the π-π* transition, and one weak absorption band in the visible region of the spectra, corresponding to the n-π* transition for all compounds of the series. As example the comparison of spectra of compounds **Ia**, **Id** and **Ih** is given in Figure 6.

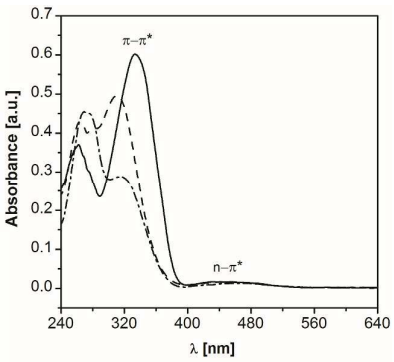

Fig. 6 UV-Vis spectra of *E*-isomers of **Ia** (solid curve), **Id** (dash and dot curve) and **Ih** (dashed curve).

Lateral substitution resulted in lowering the π-π* absorption and also to a slight blue shift of the π-π* band was observed for all materials except **Ib** (Table 4). The group of materials with faster thermal *Z*-*E* isomerization (**Ie-g**) shows more noticeable hypsochromic effect than the substances **Ib-d** with more stable *Z*-isomer. In the case of the n-π* absorption band, a small bathochromic effect of lateral substituents is observed for all compounds. All these observations are in agreement with general principles describing substituent effects on UV-Vis absorption spectra of organic compounds.[49]

Table 4 Positions of UV-Vis absorption bands of *E*-isomers of studied compounds.

comp.	λ_{max} π–π* [nm]	λ_{max} n-π* [nm]
Ia	333	431
Ib	334	474
Ic	317	471
Id	315	465
Ie	349	456
If	313	459
Ig	316	460
Ih	310	449
Ii	328	454

View Article Online
DOI: 10.1039/C6TC01103A

Upon illumination with UV-light (366 nm), typical changes in the UV spectra of all materials occur due to the gradual *E*-*Z* photoisomerization, i.e. drop of the π-π* absorption and a small increase and blue shift of the n-π* band as depicted for compound **Ib** in Figure 7.

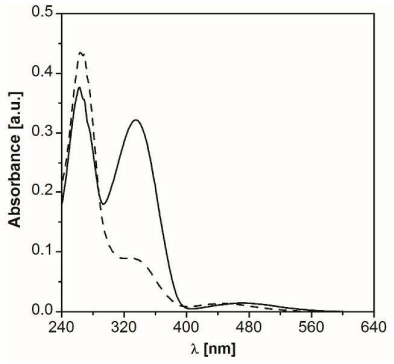

Fig. 7 UV-VIS spectra of **Ib** before (solid curve) and after (dashed curve) illumination by UV-light (366 nm) for 15 min.

Conclusion

A series of novel azo-based liquid crystalline materials has been synthesized and studied. It has been found that the thermal relaxation can be either enhanced or significantly suppressed by the same lateral substituents in different positions of the azobenzene unit. Resulting suppression of the isomerization rate is comparable to reported materials with sophisticated molecular structures designed for optical data storage. Lateral substitution also resulted in decrease of the absorption in the near UV region, compared to non-substituted parent compound **Ia**. Preservation of liquid crystalline properties is a further important feature of the studied compounds, however, the typical consequences of lateral substitution was lowering the transition temperatures and reduction of the mesomorphic polymorphism. The combination of high stability of *Z*-isomer, mesomorphic behaviour, and simple molecular structure makes derivatives **Ib-d** very good candidates for optical data storage materials. To the best of our knowledge, there have not been reported any rod-like liquid crystalline azo-materials yet which have so stable *Z*-isomers like compounds **Ib-d**.

Acknowledgements

This work was partially funded by the Czech Science Foundation (project No. 16-12150S), Ministry of Education, Youth and Sports of the Czech Republic (project MEYS LH15305) and specific university research (project MSMT No 20/2015).

References

1 A. S. Matharu, S. Jeeva, P. S. Ramanujam, *Chem. Soc. Rev.*, 2007, **36**, 1868–1880

View Article Online
DOI: 10.1039/C6TC01103A

2 T. Yamamoto, M. Hasegawa, A. Kamezawa, T. Shiono, T. Ikeda, Y. Nagase, E. Akiyama, Y. Takamura, *J. Phys. Chem. B*, 1999, **103**, 9873–9878.
3 S. Kawata, Y. Kawata, *Chem. Rev*., 2000, **100**, 1777–1788.
4 B. L. Feringa, W. R. Browne, Eds. *Molecular Switches*; Wiley-VCH: Weinheim, 2011.
5 K. D. Harris, R. Cuypers, P. Scheibe, C. L. van Oosten, C. W. M. Bastiaansen, J. Lub, D. J. Broer, *J. Mater. Chem.*, 2005, **15**, 5043–5048.
6 H. Yu, T. Ikeda, *Adv. Mater*., 2011, **23**, 2149–2180.
7 R. Shankar, T. K. Ghosh, R. J. Spontak, *Soft Matter*, 2007, **3**, 1116–1129.
8 C. Ohm, M. Brehmer, R Zentel. *Adv. Mater*. 2010, **22**, 3366–3387.
9 A. Ryabchun, A. Bobrovsky, J. Stumpe, V. Shibaev, *Adv. Optical Mater.*, 2015, **3**, 1273–1279.
10 S. Chaterji, I. K. Kwon, K. Park, *Prog. Polym. Sci.*, 2007, **32**, 1083–1122.
11 I. Tomatsu, K. Peng, A. Kros, *Adv. Drug Delivery Rev*., 2011, **63**, 1257–1266.
12 B. L. Feringa, Ed. *Molecular Switches*; Wiley-VCH: Weinheim, 2011, Ch. 12.
13 Y. Wang. Q. Li *Adv. Mater.*, 2012, **24**, 1926–1945.
14 Y. Wang. Q. Li *Adv. Funct. Mater.* 2016, **26**, 10–28.
15 Z. Zheng, Y. Li, H. K. Bisoyi, L. Wang, T. J. Bunning, Q. Li *Nature*, 2016, **531**, 352–357.
16 V. Chigrinov G., V. M. Kozenkov, H. S Kwok, *Photoalignment of Liquid Crystalline Materials: Physics and Applications (Vol. 17)*. John Wiley & Sons, 2008.
17 O. Tsutsumi, T. Kitsunai, A. Kanazawa, T. Shiono, T. Ikeda, *Macromolecules,* 1998, **31**, 355–359.
18 N. Li, J. Lu, X. Xia, Q. Xu, L. Wang, *Polymer*, 2009, **50**, 428–433.
19 H. Dürr, H. Bouas-Laurent, Eds. *Photochromism – Molecules and Systems*, Elsevier B.V., 2003.
20 T. Sasaki, T. Ikeda, *J. Phys. Chem.,* 1995, **99**, 13008–13012.
21 I. Jánossy, L. Szabados, *J. Nonlinear Opt. Phys. Mater.*, 1998, **7**, 539–551.
22 K. G. Yager, C. J. Barrett, *J. Photochem. Photobiol. A: Chemistry,* 2006, **182**, 250–261.
23 N. J. Bunce, G. Ferguson, C. L. Forber, G. J. Stachnyk, *J. Org. Chem.,* 1987, **52**, 394–398.
24 H. Rau, D. Rötger, *Mol. Cryst. Liq. Cryst.,* 1994, **246**, 143–146.
25 R. Siewertsen, H. Neumann, B. Buchheim-Stehn, R. Herges, C. Näther, F. Renth, F. Temps, *J. Am. Chem. Soc*., 2009, **131**, 15594–15595.
26 Y. Norikane, R. Katoh, N. Tamaoki, *Chem. Commun*., 2008, 1898–1900.
27 P. J. Collings, M. Hird, *Introduction to Liquid Crystals*. Taylor & Francis, London, 1997.
28 M. Kašpar, A. Bubnov, V. Hamplová, S. Pirkl, M. Glogarová, *Liq. Cryst.*, 2004, **31**, 821–830.
29 H. M. D. Bandara, S. C. Burdette, *Chem. Soc. Rev.*, 2012, **41**, 1809–1825.

30 F.-N. Li, N.-J. Kim, D.-J. Chang, J. Jang, H. Jang, J.-W. Jung, K.-H. Min, Y.-S. Jeong, S.-Y. Kim, Y.-H. Park, H.-D. Kim, H.-G. Park, Y.-G. Suh, *Bioorg. Med. Chem*., 2009, **17**, 8149–8160.
31 R. Hartmann, M. Frotscher, S. Oberwinkler, E. Ziegler, J. Messinger, H. H. Thole, US Patent App. US20100204234 A1, Aug 12, 2010.
32 R. Willstätter, G. Schudel, *Ber. Dtsch. Chem. Ges*., 1918, **51**,782–788.
33 J. Dokić, M. Gothe, J. Wirth, M. V. Peters, J. Schwarz, S. Hecht, P. Saalfrank, *J. Phys. Chem. A*, 2009, **113**, 6763–6773A.
34 C. Hansch, A. Leo, R. W. Taft, *Chem. Rev.* 1991, **91**, 165-195.

35 Altomare, L. Andruzzi, F. Ciardelli, R. Solaro, N. Tirelli, *Macromol. Chem. Phys*., 1999, **200**, 601–608.

View Article Online
DOI: 10.1039/C6TC01103A

36 Y. Norikane, K. Kitamoto, N. Tamaoki, *J. Org. Chem.,* 2003, **68**, 8291–8304.
37 D. Röttger, H. Rau, *J. Photochem. Photobiol. A. Chemistry,* 1996, **101**, 205–214.
38 Y. Shirota, K. Moriwaki, S. Yoshikawa, T. Ujike, H. Nakano, *J. Mater. Chem*., 1998, **8**, 2579–2581.
39 M. S. Vollmer, T. D. Clark, C. Steinem, M. R. Ghadiri, *Angew. Chem. Int. Ed*., 1999, **38**, 1598–1601.
40 M. Müri, K. C. Schuermann, L. De Cola, M. Mayor, *Eur. J. Org. Chem.,* 2009, 2562–2575.
41 S. A. Nagamani, Y. Norikane, N. Tamaoki, *J. Org. Chem.* 2005, **70**, 9304–9313.
42 A. A. Beharry, O. Sadovski, G. A. Woolley, *J. Am. Chem. Soc.*, 2011, **133**, 19684–19687.
43 A. Bobrovsky, A. Ryabchun, M. Cigl, V.Hamplová, M. Kašpar, F. Hampl, V. Shibaev, *J. Mater. Chem. C*, 2014, **2**, 8622.
44 A. Bobrovsky, V. Shibaev, A. Bubnov, V. Hamplová, M. Kašpar, M. Glogarová, *Macromolecules*, 2013, **46**, 4276–4284.
45 A. Bubnov, V. Hamplová, M. Kašpar, P. Vaněk, D. Pociecha, M. Glogarová, *Mol. Cryst. Liq. Cryst. Sci. Technol., Sect. A*, 2001, **366**, 547–556.
46 M. Kašpar, V. Hamplová, S.A. Pakhomov, I. Stibor, H. Sverenyák, A. Bubnov, M. Glogarová, P. Vaněk, *Liq. Cryst.*, 1997, **22**, 557–561.
47 M. Kašpar, A. Bubnov, V. Hamplová, Z. Málková, S. Pirkl, M. Glogarová, *Liq. Cryst.*, 2007, **34**, 1185–1192.
48 V. Novotná, V. Hamplová, A. Bubnov, M. Kašpar, M. Glogarová, N. Kapernaum, S. Bezner, F. Giesselmann, *J. Mater. Chem.*, 2009, **19**, 3992–3997.
49 O. H. Wheeler; P. Gore. *Org. Chem*., 1961, **26**, 3295–3298.